S/X Band Experiment: A Study of the Effects of Multipath on Two-Way Range

T. Y. Otoshi
Communications Elements Research Section

Equations are presented for determining two-way range errors caused by multipath. The analysis of two-way range error is more complex than that for one-way range due to the fact that the uplink and downlink range errors oscillate at different rates when the leakage path length is varied. A limited amount of two-way range data was obtained with the Mu-1 ranging machine, Mariner Venus/Mercury 1973 Radio Frequency Subsystem, and Block 3 receiver. The agreement between theoretical and experimental values was typically better than 2 ns.

I. Introduction

In this article, the term "one-way" range will be used to refer to either uplink or downlink range while the term "two-way" range will be used to refer to the sum of the uplink and downlink ranges. For the S/X band experiment the uplink frequency transmitted to the spacecraft transponder was 2113 MHz, while coherent S/X band downlink frequencies transmitted back to the ground station were 2295 and 8415 MHz. In a dispersive media, the two-way range will not generally be equal to twice the one-way range.

The analysis of the effects of multipath on one-way range was presented previously by this author in Ref. 1 and by J. R. Smith in Ref. 2. Theoretical equations for one-way range errors were verified experimentally by use of a multipath device, MVM'73 Radio Frequency Subsystem, Block 3 receiver/exciter subsystem (RCV) and the Mu-1 ranging machine.

This report presents theoretical equations which can be used to analyze the effects of multipath on two-way range. In addition, some experimental data, which show good agreement with the theory, will be presented.

II. Theoretical Equations

A. Exact Formulas

The geometry for two-way range error analysis may be seen in Fig. 1. For this geometry the two-way range error is simply the algebraic sum of the one-way range error for the uplink signal and the one-way range error for the downlink signal.

The equation for two-way range can be expressed as

$$(t_g)_T = (t_{g1})_a + (t_{g1})_b + \epsilon_{ga} + \epsilon_{gb} \tag{1}$$

and the two-way range error as

$$(\epsilon_g)_T = \epsilon_{ga} + \epsilon_{gb} \tag{2}$$

where

$(t_{g1})_a$ = group delay of the uplink signal in the absence of multipath, s

$(t_{g1})_b$ = group delay of the downlink signal in the absence of multipath, s

ϵ_{ga} = error in the uplink delay due to multipath, s

ϵ_{gb} = error in the downlink delay due to multipath, s

For simplicity, assume that the primary and leakage paths are the same for the uplink and downlink signals (Fig. 1). Then from the equations derived in Ref. 1, and assuming a free-space media for both leakage and primary paths

$$\epsilon_{ga} = \frac{(\ell_2 - \ell_1)}{c} A \left(\frac{A + \cos\theta_a}{1 + 2A\cos\theta_a + A^2}\right) \tag{3}$$

$$\epsilon_{gb} = \frac{(\ell_2 - \ell_1)}{c} A \left(\frac{A + \cos\theta_b}{1 + 2A\cos\theta_b + A^2}\right) \tag{4}$$

where

$$\theta_a = \frac{-2\pi f_a}{c}(\ell_2 - \ell_1) + \psi_a \tag{5}$$

$$\theta_b = \frac{-2\pi f_b}{c}(\ell_2 - \ell_1) + \psi_b \tag{6}$$

and

A = ratio of the magnitudes of the leakage and primary signals as measured at the input port to the transponder (Fig. 1)

ℓ_1, ℓ_2 = physical path lengths, respectively, of the primary and leakage paths going one-way, m

c = speed of light ($\simeq 3 \times 10^8$ m/s)

f_a, f_b = uplink and downlink frequencies, respectively, in Hz

ψ_a, ψ_b = phase angles of reflection coefficients (if any) in the leakage path for uplink and downlink signals, respectively, in radians

The terms ψ_a and ψ_b in Eqs. (5) and (6) have been added for generality. It is assumed that the reflection coefficient phase angles do not change with frequency over the frequency interval of interest and, therefore, only affect the location of the upper and lower bounds of range error (see Appendix A).

It is also of interest to examine the effects of multipath on the AGC signal level as observed on the ground receiver. If the transponder is similar to that of the MVM'73 spacecraft where the downlink output signal of the transponder is kept constant even if the uplink signal is varying, then the AGC signal level error at the ground receiver will vary according to the relationship. (Ref. 1):

$$|F_b|_{\text{dB}} = 10\log_{10}[1 + 2A\cos\theta_b + A^2] \tag{7}$$

If the transponder is a translator or a zero delay device, the AGC signal level error measured at the ground receiver will vary according to the relationship

$$|F_T|_{\text{dB}} = 10\log_{10}[(1 + 2A\cos\theta_a + A^2)(1 + 2A\cos\theta_b + A^2)] \tag{8}$$

B. Approximate Formulas

The exact equations presented above are somewhat difficult to analyze because the uplink and downlink phases change at different rates. In the cases of small leakage one can make approximations which show a type of modulation effect produced by the uplink and downlink error functions adding together. If x represents the terms having factors of A in the denominators of Eqs. (3) and (4) one can use the small x approximation that $(1 + x)^{-1} \approx 1 - x$. Then, from substitutions into Eq. (2), omitting higher order terms of A after multiplication and the use of trigonometric identities, one obtains the approximate formula

$$\begin{aligned}(\epsilon_g)_T &\approx A\left(\frac{\ell_2 - \ell_1}{c}\right) \times [\cos\theta_a + \cos\theta_b - A(\cos 2\theta_a + \cos 2\theta_b)] \\ &\approx 2A\left(\frac{\ell_2 - \ell_1}{c}\right)\left[\cos\frac{1}{2}(\theta_b - \theta_a)\cos\frac{1}{2}(\theta_b + \theta_a) - A\cos(\theta_b - \theta_a)\cos(\theta_b + \theta_a)\right]\end{aligned} \tag{9}$$

The accuracy of the above approximate formula is better than 3% if $A \leq 0.1$. If the difference between the uplink and downlink signals is small, then the error curves will be similar to an amplitude-modulated signal where the envelope of the modulation is proportional to cos $[(1/2)(\theta_b - \theta_a)]$ and the carrier signal is given by cos $[(1/2)(\theta_b + \theta_a)]$.

Similarly, when the small leakage signal approximations are used in Eq. (8), the following approximate formula is obtained

$$|F_T|_{\mathrm{dB}} \simeq 10 \log_{10} \left[1 + 4A \cos \frac{1}{2}(\theta_b - \theta_a) \cos \frac{1}{2}(\theta_b + \theta_a) \right] \tag{10}$$

C. Sample Cases

Figures 2 through 13 are sample case plots of Eqs. (2) and (8) for leakage signal levels of −30 dB, −20 dB, and −10 dB relative to the primary signal. Figures 2 through 7 are plots applicable for 2113-MHz uplink and 2295-MHz downlink cases, while Figs. 8 through 13 are applicable to 2113-MHz uplink and 8415-MHz downlink cases. For these sample cases, the leakage path is initially assumed to be 3048 cm (100 ft) longer than the primary path. Then the leakage path is increased and errors are plotted as a function of increasing differential path lengths. Error curves for other differential path lengths will be similar in shape, but the amplitudes will differ by the ratio of the differential path lengths. At some critical differential path length the errors become worst case, and the upper and lower bounds will be twice those for one-way range. (See Appendix A.)

In the sample case plots it is of interest to note the similarity of the periodicity and shapes of the range and signal level error curves. This fact can be used to advantage, as will be described in the following suggested experiment.

D. Application

Although the two-way theory is complex, the multipath effects can be separated out in practice. Picture an experimental setup where the zero delay device horn is moved along the direction of the primary path. Measurements of the signal level and range are simultaneously recorded as a function of the zero delay device horn position. To obtain at least two cycles of change, the S-band zero delay horn should be moved a minimum of 27.2 cm (10.7 in.) while at X-band, the ZDD horn should be moved at least 11.4 cm (4.5 in.). After the experimental data has been obtained, a curve fit can be made to the experimental AGC signal level data using Eq. (8). Then determining the position at which the signal level amplitude error is zero, it can be assumed that at the same position the two-way range error is also zero (Figs. 2 to 13). This procedure should produce an error of only a few nanoseconds if the peak-to-peak AGC signal level change is less than 2 dB. For larger AGC ripples (indicating severe multipath conditions) a curve fit of experimental data should be made to both theoretical range and signal level equations given by Eqs. (2) and (8).

III. Experimental Verification

Ranging tests were performed at the Telecommunications Development Laboratory (TDL) using the Block 3 RCV, MVM'73 Radio Frequency Subsystem, and the MU-1 ranging machine. The multipath device[1] described in Ref. 1 was inserted into a cable path that simultaneously carried both the uplink 2113 MHz and downlink 2295 MHz range-coded signals. A block diagram of the test setup at TDL may be seen in Fig. 14. For the two-way range tests, the initial test parameters of the Block 3 RCV and MU-1 ranging machine were the same as previously reported in Ref. 1.

A cable of the appropriate length was inserted into the leakage path of the multipath device to make the one-way leakage path delay become 22.8 ns longer than the delay through the primary path. The multipath device attenuator was adjusted so that the one-way leakage signal was −10.55 dB relative to the primary signal. The leakage path length was then varied by means of a phase shifter (line stretcher) in the leakage path. Two-way range changes and received signal level were measured as functions of the phase shifter setting.

Table 1 shows a comparison of experimental and theoretical values. The theoretical two-way range values were computed from Eq. (2). It can be seen that the agreement between theoretical and experimental range values were typically better than 2 ns. From Table 1 it can also be seen that the theoretical values of signal level changes agreed with experimental values to within 0.5 dB. Eq. (7) was used for the theoretical values for signal level changes because the MVM'73 radio-frequency subsystem transponder was used for these tests rather than a zero delay device. Although it is known that the group delay of the spacecraft receiver system changes as a function of received uplink signal level, no attempt was made to correct the experimental data for these changes.

[1]The isolators in the multipath device were replaced by short lengths of Uniform Tubes UT141 semi-rigid cables.

IV. Conclusion

Equations for two-way range error due to multipath have been presented. Although only a limited amount of experimental data was obtained, reasonably good agreement was found between theory and experiment.

For a future experiment with a dish-mounted zero-delay device, one could mount a zero-delay horn on rails and then record two-way signal level and range changes as a function of horn position. With this data a correlation analysis can be made between experimental data and the theoretical equations. This should enable determination of the true range which would be obtained in the absence of multipath. It should be pointed out that this experimental procedure would be valid only if the multipath phenomenon is caused by one dominant leakage signal. If there are multiple leakage signals, the present analysis would have to be made more general.

Table 1. Results of two-way range test with the multipath device (Uplink frequency = 2.113 GHz, downlink frequency = 2.295 GHz)

Phase shifter setting	$\ell_2 - \ell_1$, cm	Range change			Downlink signal level change		
		Measured[a], ns	Theoretical[b], ns	Difference, ns	Measured, dB	Theoretical, dB	Difference, dB
0	684.00	0.00	0.00	0.00	—	+1.11	—
10	684.83	− 5.27	− 5.13	−0.14	0.00	0.0	0.00
20	685.67	−10.44	−10.81	0.37	—	−0.85	—
30	686.50	−14.75	−14.70	−0.05	−1.54	−1.03	−0.51
40	687.33	−15.75	−15.66	−0.09	−1.09	−0.45	−0.64
50	688.17	−15.09	−14.59	−0.50	−0.02	0.59	−0.61
60	689.00	−12.23	−11.38	−0.85	+1.19	1.71	−0.52
70	689.83	− 8.22	− 6.36	−1.86	—	2.68	—
80	690.67	− 4.32	− 1.31	−3.01	2.97	3.44	−0.47
90	691.50	0.16	2.57	−2.41	3.48	3.95	−0.47
100	692.33	2.34	5.15	−2.81	3.77	4.22	−0.45
110	693.17	4.21	6.63	−2.42	3.83	4.23	−0.40
120	694.00	5.45	7.20	−1.75	3.65	4.01	−0.36
130	694.83	5.10	6.93	−1.83	3.24	3.53	−0.29
140	695.67	4.29	5.76	−1.47	—	2.81	—
150	696.50	2.14	3.48	−1.34	1.54	1.86	−0.32
160	697.33	− 1.79	− 0.14	−1.65	0.37	0.76	−0.39
170	698.17	− 6.43	− 4.96	−1.47	—	−0.31	—
180	699.00	−10.74	− 9.42	−1.32	—	−0.99	—

[a]Calculated standard error on the measured relative range was typically ±0.5 ns

[b]Based on $A = 0.297$ (-10.55 dB)

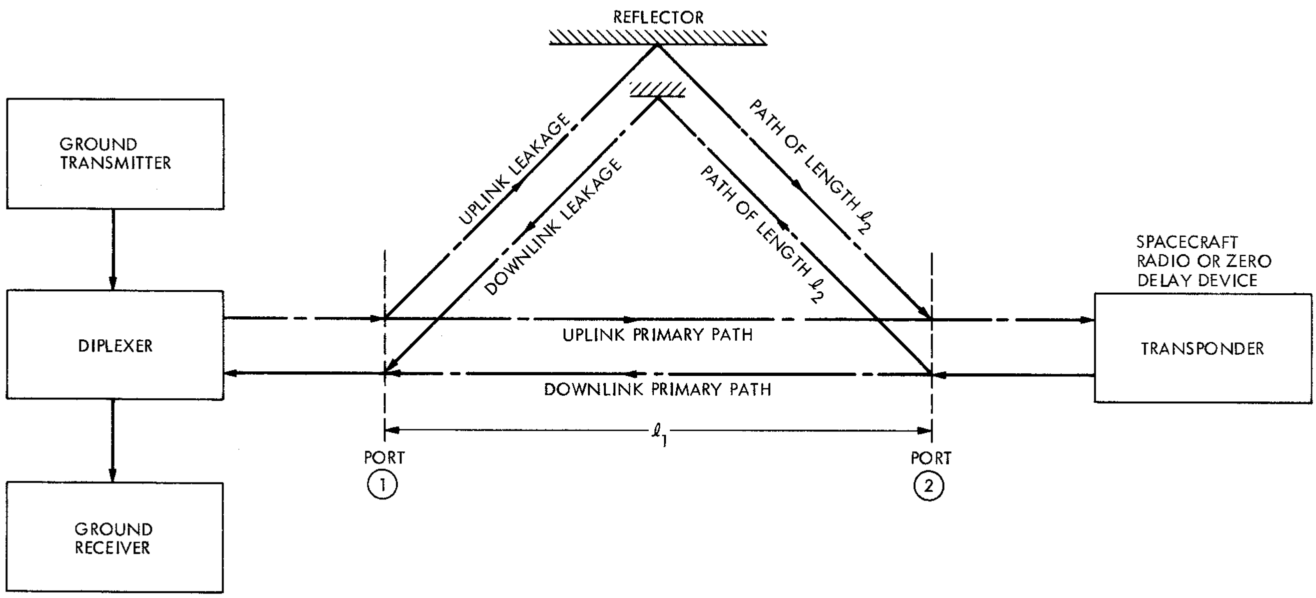

Fig. 1. Geometry for analysis of the effect of multipath on two-way range

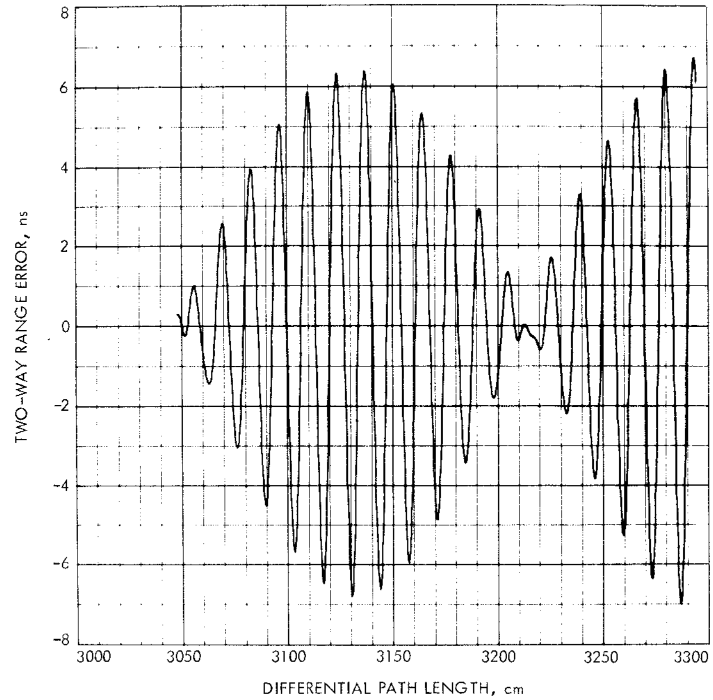

Fig. 2. Two-way *range* error sample case: $\ell_2 - \ell_1 = 3048$ cm (100 ft); one-way leakage signal is -30 dB relative to primary signal; uplink signal is 2113 MHz, and downlink signal is 2295 MHz; $\psi_a = \psi_b = 0$

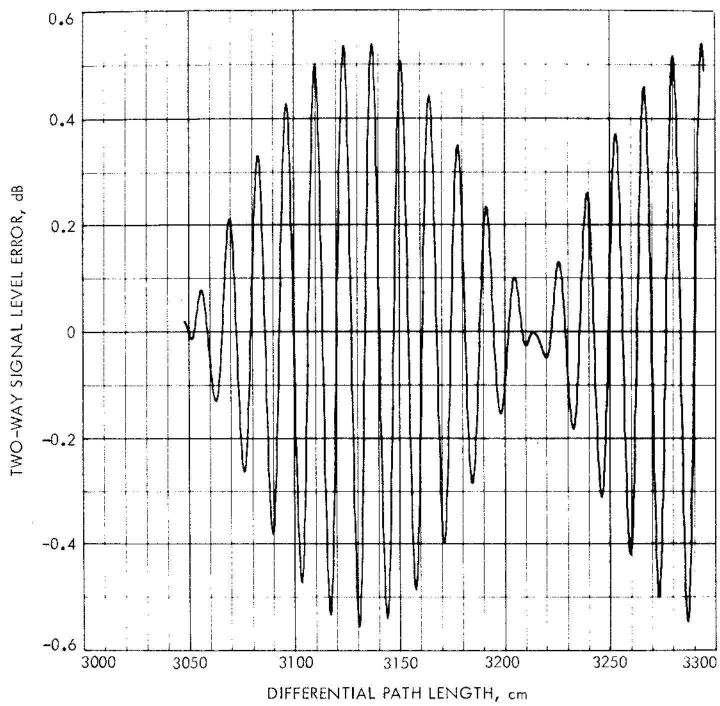

Fig. 3. Two-way *signal* level error sample case (same parameters as Fig. 2)

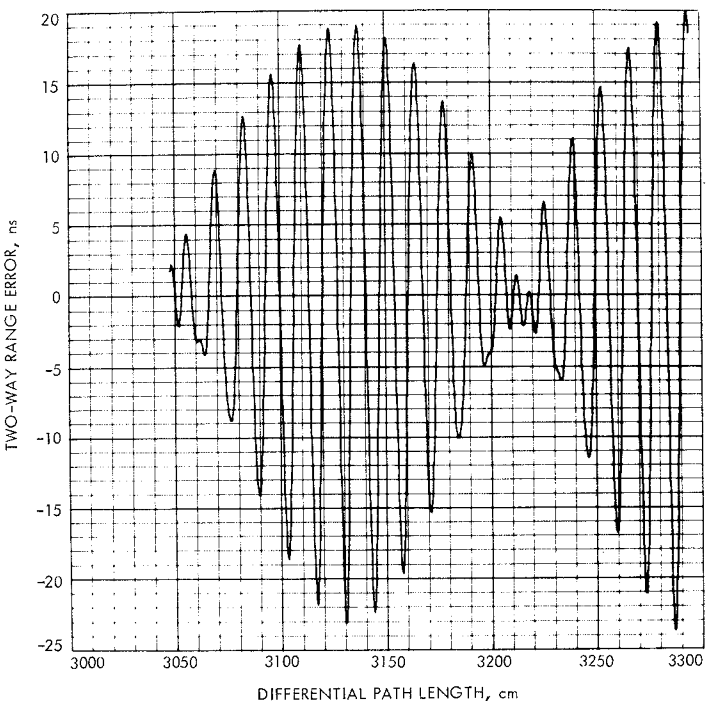

Fig. 4. Two-way *range* error sample case: same parameters as Fig. 2 except leakage signal is −20 dB relative to primary signal

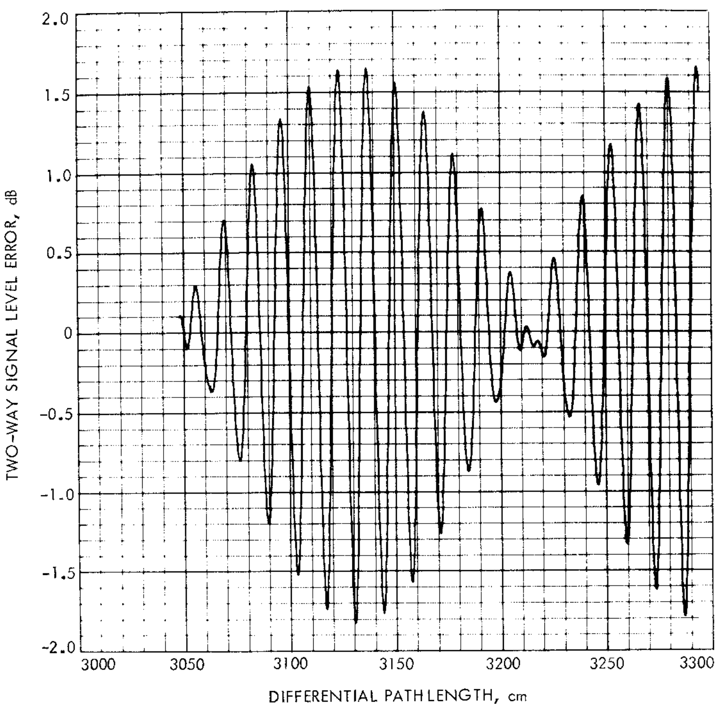

Fig. 5. Two-way *signal* level error sample case: same parameters as Fig. 2 except leakage signal is −20 dB relative to primary signal

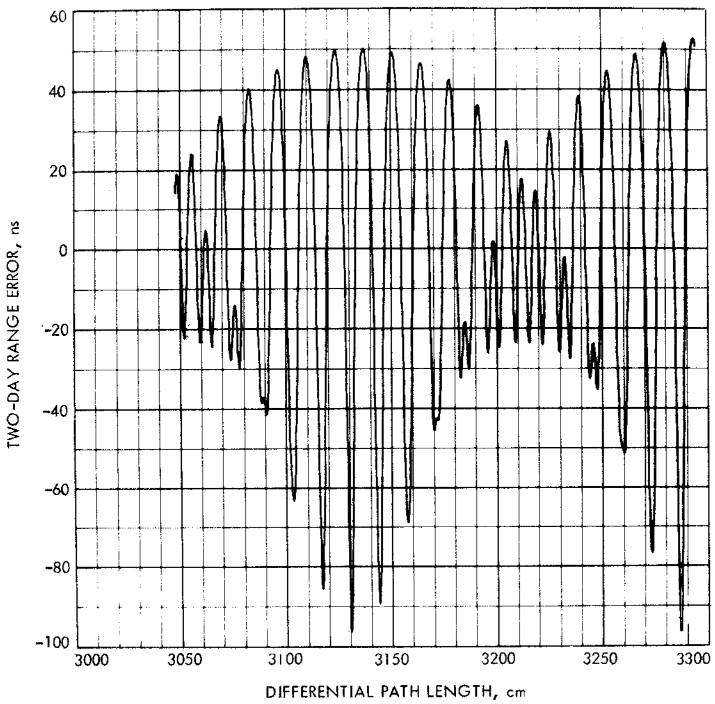

Fig. 6. Two-way *range* error sample case: same parameters as Fig. 2 except leakage signal is −10 dB relative to primary signal

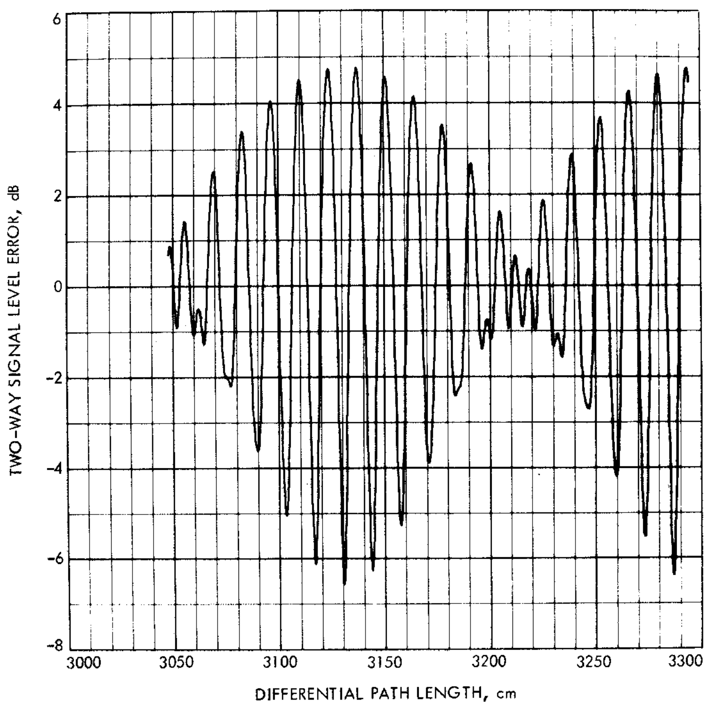

Fig. 7. Two-way *signal* level error sample case: same parameters as Fig. 2 except leakage signal is −10 dB relative to primary signal

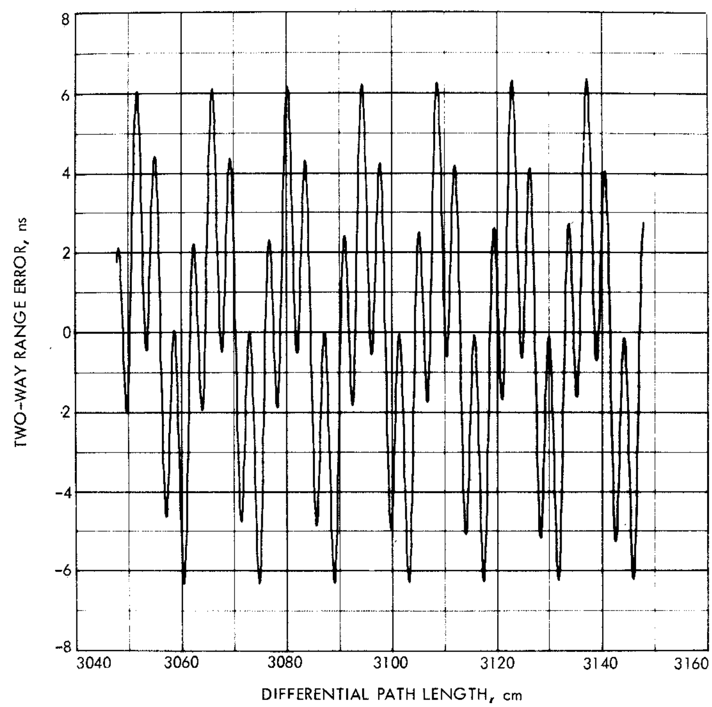

Fig. 8. Two-way *range* error sample case: $\ell_2 - \ell_1 = 3048$ cm (100 ft); one-way leakage signal is -30 dB relative to primary signal; uplink signal is 2113 MHz, and downlink signal is 8415 MHz; $\psi_a = \psi_b = 0$

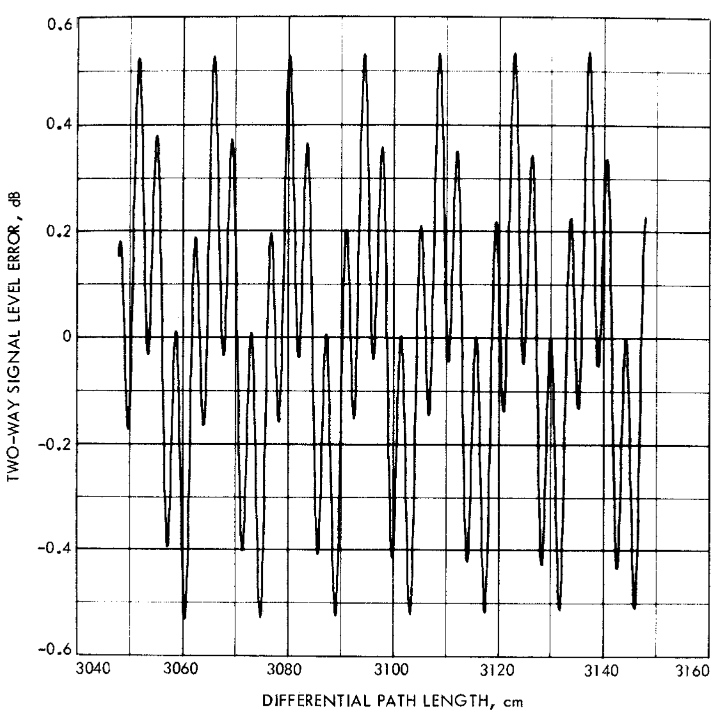

Fig. 9. Two-way *signal* level error sample case (same parameters as Fig. 8)

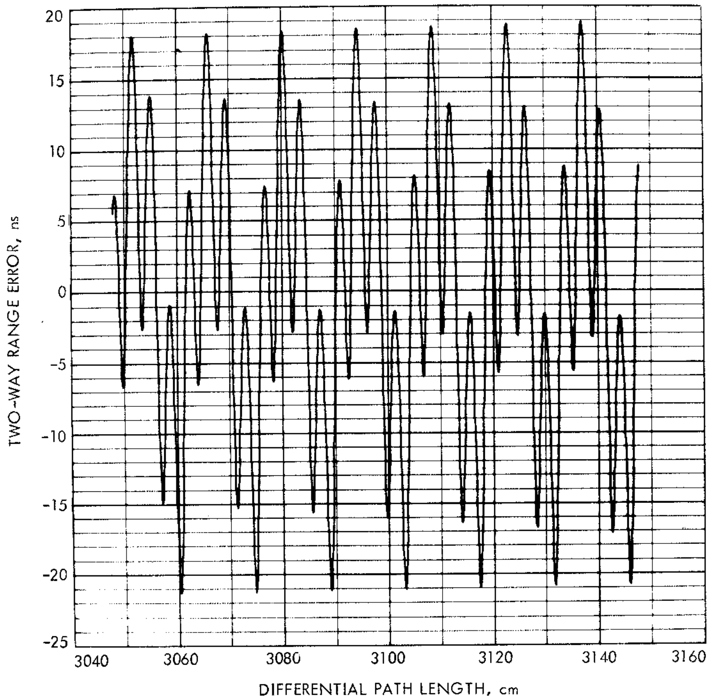

Fig. 10. Two-way *range* error sample case: same parameters as Fig. 8 except leakage signal is −20 dB relative to primary signal

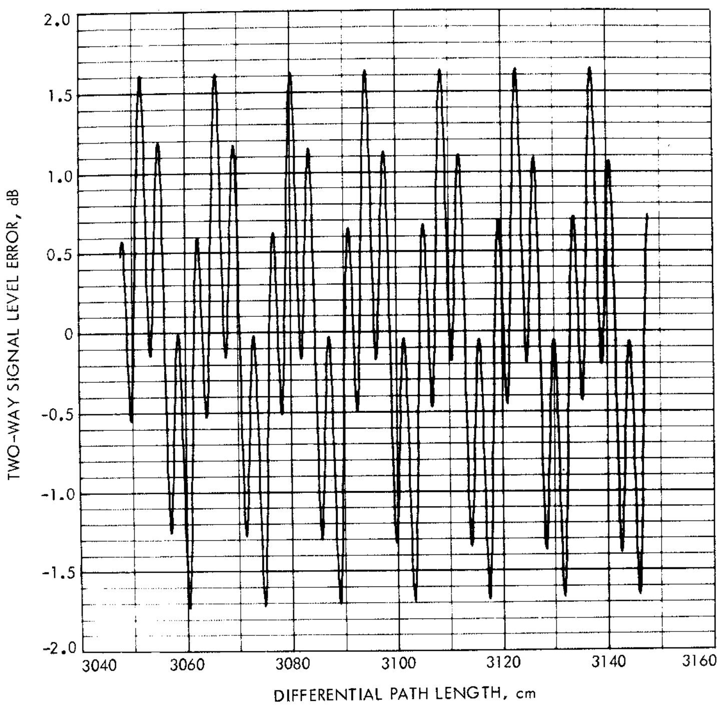

Fig. 11. Two-way *signal* level error sample case: same parameters as Fig. 8 except leakage signal is −20 dB relative to primary signal

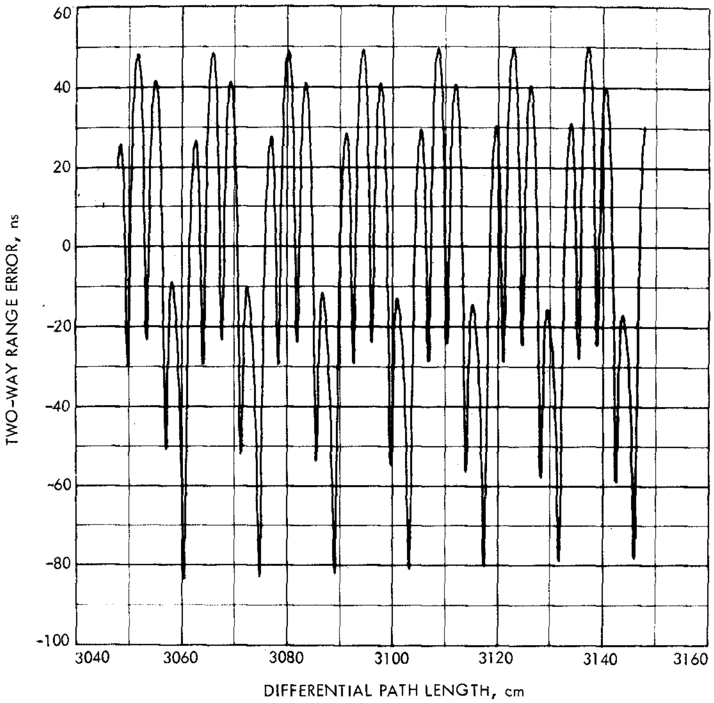

Fig. 12. Two-way *range* error sample case: same parameters as Fig. 8 except leakage signal is −10 dB relative to primary signal

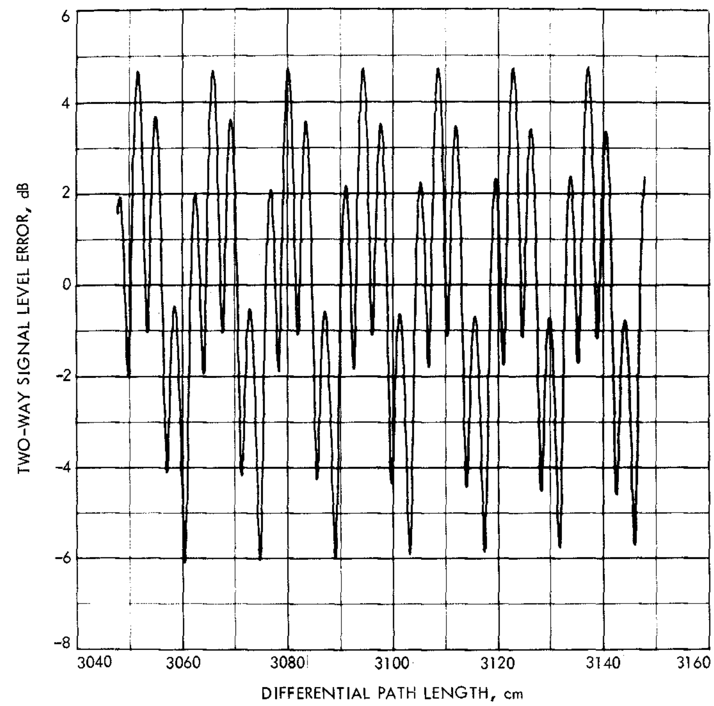

Fig. 13. Two-way *signal* level error sample case: same parameters as Fig. 8 except leakage signal is −10 dB relative to primary signal

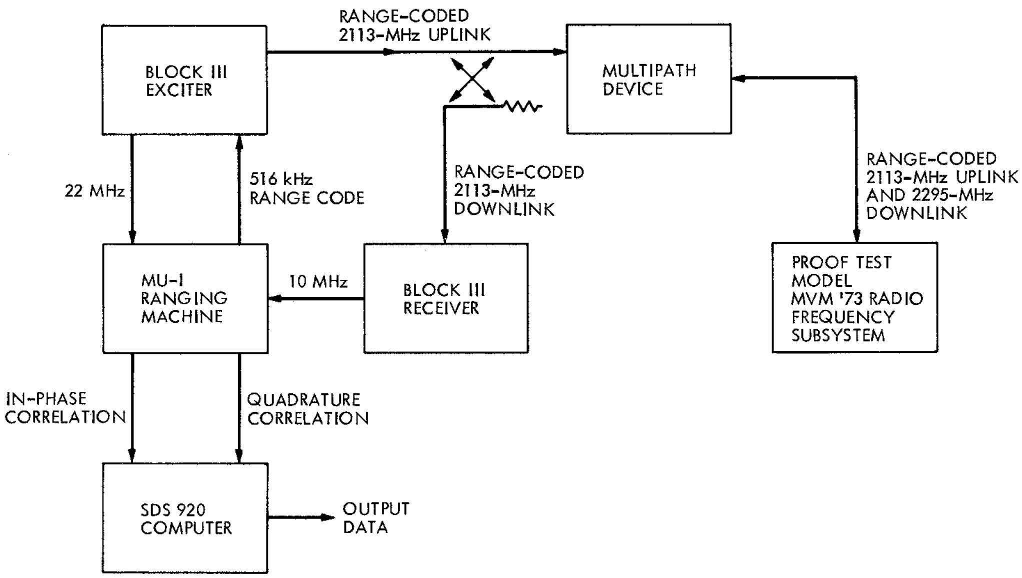

Fig. 14. Measurement setup for two-way range tests with the multipath device

Appendix A

Upper and Lower Bounds for Two-Way Range Error

As can be seen from the sample case plots (Figs. 2 to 13), the error for two-way range will be at a *local* upper or lower bound when the modulation envelope is at a maximum or minimum. At some critical differential path length, the two-way range error will be exactly two times the upper or lower bound of the one-way range error (Ref. 1). To find where this condition occurs, let θ_a and θ_b as given by Eqs. (5) and (6) be related as follows

$$\theta_b = \theta_a - 2\pi k \tag{A-1}$$

where k is a positive integer. Then the two-way range error given by Eq. (2) becomes

$$(\epsilon_g)_T = 2A\left(\frac{\ell_2 - \ell_1}{c}\right)\left(\frac{A + \cos\theta_a}{1 + 2A\cos\theta_a + A^2}\right) \tag{A-2}$$

Also note that the two-way signal level error as given by Eq. (8) becomes

$$|F_T|_{\mathrm{dB}} = 20\log_{10}[1 + 2A\cos\theta_a + A^2] \tag{A-3}$$

From Eq. (A-3), it can be seen that the peak-to-peak change in signal level will be

$$\Delta_{\mathrm{dB}} = 40\log_{10}\left[\frac{1 + A}{1 - A}\right] \tag{A-4}$$

which is exactly a factor of two greater than the dB signal level ripple for the one-way case (Ref. 1).

Upper Bound

Assuming that the conditions of Eq. (A-1) exist, then assume further that

$$\theta_a = -2\pi m \tag{A-5}$$

where m is a positive integer. Substitution of Eq. (A-5) into Eqs. (A-2) and (A-3) gives

$$(\epsilon_g)_T = \left(\frac{2A}{1 + A}\right)\left(\frac{\ell_2 - \ell_1}{c}\right) \tag{A-6}$$

$$|F_T|_{\mathrm{dB}} = 40\log_{10}(1 + A) \tag{A-7}$$

These upper bounds of error for two-way range and signal level are exactly twice those of the corresponding one-way range case (Ref. 1). To find the critical differential path length which produces these conditions, first substitute Eq. (A-5) into (A-1) to obtain

$$\theta_b = -2\pi(m + k) \tag{A-8}$$

Then substitutions of Eqs. (5) and (6) into Eqs. (A-5) and (A-8), respectively, and solving for $\ell_2 - \ell_1$ results in

$$\ell_2 - \ell_1 = \left(\frac{c}{f_a}\right)\left[m + \frac{\psi_a}{2\pi}\right] \tag{A-9}$$

$$\ell_2 - \ell_1 = \left(\frac{c}{f_b}\right)\left[m + k + \frac{\psi_b}{2\pi}\right] \tag{A-10}$$

For simplicity assume that there is only one reflection coefficient in the leakage path and $\psi_a = \psi_b = \pi$. Then equating Eq. (A-9) to Eq. (A-10) and manipulation results in

$$f_b = f_a\left[\frac{2(m + k) + 1}{2m + 1}\right] \tag{A-11}$$

The condition of Eq. (A-11) must be fulfilled if two-way range error is exactly twice the one-way range value. To show a practical application of Eq. (A-11), one can find from trial and error that $m = 11$ and $k = 1$ are the minimum values of m and k which will give $f_b \simeq 2295$ MHz when $f_a = 2113$ MHz. From substitution of these values in Eqs. (A-11) and (A-9)

$$f_b = 2296.7 \text{ MHz}$$

$$\ell_2 - \ell_1 = 163.3 \text{ cm (5.36 ft)}$$

and from Eq. (A-6)

$$(\epsilon_g)_T = 10.89\left(\frac{A}{1 + A}\right)$$

where $(\epsilon_g)_T$ is given in nanoseconds.

Lower Bound

To find where the two-way lower bound is exactly twice the one-way lower bound, assume that the condition of Eq. (A-1) exists, and assume further that

$$\theta_a = -(2n - 1)\pi \tag{A-12}$$

where n is a positive integer. Then Eqs. (A-2) and (A-3) become

$$(\epsilon_g)_T = -\left(\frac{2A}{1-A}\right)\left(\frac{\ell_2 - \ell_1}{c}\right) \tag{A-13}$$

$$|F_T|_{\text{dB}} = 40 \log_{10} [1 - A] \tag{A-14}$$

To find the differential path length which produces these lower bounds, substitute Eq. (A-12) into Eq. (A-1) to obtain

$$\theta_b = -(2n - 1)\pi - 2\pi k \tag{A-15}$$

Then substitutions of Eqs. (5) and (6) into Eqs. (A-12) and (A-15), respectively, and then solving for $\ell_2 - \ell_1$ results in

$$\ell_2 - \ell_1 = \frac{c}{f_a}\left[\left(\frac{2n-1}{2}\right) + \frac{\psi_a}{2\pi}\right] \tag{A-16}$$

$$\ell_2 - \ell_1 = \frac{c}{f_b}\left[\left(\frac{2n-1+2k}{2}\right) + \frac{\psi_b}{2\pi}\right] \tag{A-17}$$

Assuming that $\psi_a = \psi_b = \pi$ and then from equating Eq. (A-16) to Eq. (A-17), one obtains

$$f_b = f_a\left[\frac{n+k}{n}\right] \tag{A-18}$$

As an example of the use of Eq. (A-18) one can find from trial and error that values of $n = 23$ and $k = 2$ will give $f_b \simeq 2295$ MHz when $f_a = 2113$ MHz. From substitutions of these values into Eqs. (A-18) and (A-16), one obtains

$$f_b = 2296.7 \text{ MHz}$$

$$\ell_2 - \ell_1 = 326.5 \text{ cm } (10.71 \text{ ft})$$

and from Eq. (A-13):

$$(\epsilon_g)_T = -21.77\left(\frac{A}{1-A}\right)$$

where $(\epsilon_g)_T$ is given in nanoseconds.

Although in the examples given, the calculated downlink frequency of 2296.7 MHz is only approximately equal to 2295 MHz, one can expect to find local upper and lower bounds at differential path lengths close to 163.3 cm (5.36 ft) and 326.5 cm (10.71 ft). It is of interest to note that even for these small differential path length values, significant error in the S-band two-way range will occur if the multipath signal is strong. This type of strong multipath effect for small differential path lengths on the MVM'73 spacecraft was pointed out by J. R. Smith (Ref. 3).

Acknowledgments

The experimental work at the Telecommunications Development Laboratory was supported by D. L. Brunn of the Spacecraft Radio Section. The computer program for the sample case plots in this article was written by T. Cullen of the Communications Elements Research Section.

References

1. Otoshi, T. Y., "S/X Band Experiment: A Study of the Effects of Multipath on Group Delay," in *The Deep Space Network Progress Report 42-24*, pp. 40–50, Pasadena, Calif., Dec. 15, 1974.

2. Smith, J. R., "Viking Ranging Investigation Team," IOM 3382-74-076, July 30, 1974 (JPL internal document).

3. Smith, J. R., "Viking Ranging Investigation Team," IOM 3382-74-102, Oct. 15, 1974 (JPL internal document).